

Tuning the diffusion constant to optimize the readout of positional information of spatial concentration patterns

Ka Kit Kong(江嘉杰), Chunxiong Luo(罗春雄), and Feng Liu(刘峰)

Citation: Chin. Phys. B, 2024, 33 (**8**): 088703. DOI: 10.1088/1674-1056/ad4cda

What follows is a list of articles you may be interested in

Dynamics of information diffusion and disease transmission in time-varying multiplex networks with asymmetric activity levels

Xiao-Xiao Xie(谢笑笑), Liang-An Huo(霍良安), Ya-Fang Dong(董雅芳), and Ying-Ying Cheng(程英英)

Chin. Phys. B, 2024, 33 (**3**): 038704. DOI: 10.1088/1674-1056/ad1176

Studying the co-evolution of information diffusion, vaccination behavior and disease transmission in multilayer networks with local and global effects

Liang'an Huo(霍良安) and Bingjie Wu(武兵杰)

Chin. Phys. B, 2024, 33 (**3**): 038702. DOI: 10.1088/1674-1056/ad0114

Characteristics of cell motility during cell collision

Yikai Ma(马一凯), Na Li(李娜), and Wei Chen(陈唯)

Chin. Phys. B, 2024, 33 (**2**): 028702. DOI: 10.1088/1674-1056/ad117c

Heterogeneous hydration patterns of G-quadruplex DNA

Cong-Min Ji(祭聪敏), Yusong Tu(涂育松), and Yuan-Yan Wu(吴园燕)

Chin. Phys. B, 2023, 32 (**2**): 028702. DOI: 10.1088/1674-1056/ac7452

Characteristics analysis of acupuncture electroencephalograph based on mutual information Lempel–Ziv complexity

Luo Xi-Liu(罗昔柳), Wang Jiang(王江), Han Chun-Xiao(韩春晓), Deng Bin(邓斌), Wei Xi-Le(魏熙乐), and Bian Hong-Rui(边洪瑞)

Chin. Phys. B, 2012, 21 (**2**): 028701. DOI: 10.1088/1674-1056/21/2/028701

Tuning the diffusion constant to optimize the readout of positional information of spatial concentration patterns

Ka Kit Kong(江嘉杰)[1], Chunxiong Luo(罗春雄)[1,2,3], and Feng Liu(刘峰)[4,†]

[1] *The State Key Laboratory for Artificial Microstructures and Mesoscopic Physics, School of Physics, Peking University, Beijing* 100871, *China*
[2] *Center for Quantitative Biology, Peking University, Beijing* 100871, *China*
[3] *Wenzhou Institute University of Chinese Academy of Sciences, Wenzhou* 325001, *China*
[4] *Key Laboratory of Hebei Province for Molecular Biophysics, Institute of Biophysics, School of Health Science & Biomedical Engineering, Hebei University of Technology, Tianjin* 300130, *China*

(Received 8 April 2024; revised manuscript received 7 May 2024; accepted manuscript online 17 May 2024)

Positional information encoded in spatial concentration patterns is crucial for the development of multicellular organisms. However, it is still unclear how such information is affected by the physically dissipative diffusion process. Here we study one-dimensional patterning systems with analytical derivation and numerical simulations. We find that the diffusion constant of the patterning molecules exhibits a nonmonotonic effect on the readout of the positional information from the concentration patterns. Specifically, there exists an optimal diffusion constant that maximizes the positional information. Moreover, we find that the energy dissipation due to the physical diffusion imposes a fundamental upper limit on the positional information.

Keywords: pattern formation, positional information, mutual information, diffusion

PACS: 87.18.Hf, 87.19.lo, 87.15.Vv **DOI:** 10.1088/1674-1056/ad4cda

1. Introduction

In multicellular organisms, cells need to differentiate or express different genes according to their positions for precise development.[1] To provide positional information, spatial concentration patterns such as morphogen gradients are often employed.[2–7] Generally, in the presence of a spatially heterogeneous concentration distribution of a certain molecule such as a morphogen, cells can infer their positions based on the readout of the local concentration of such a molecule.[1,2,8–11] Various mechanisms for establishing nonuniform distribution of molecules have been extensively studied, e.g., the Turing mechanism,[12,13] the wave-pinning (WP) model,[14] the active transport (AT) model,[15–17] and the synthesis-degradation-diffusion (SDD) model.[4,7,18] The Turing mechanism usually involves two mutually interacting molecular species with strong nonlinearity and distinct diffusion constants, leading to the Turing instability, i.e., the destabilization of uniform concentration distribution.[12,13] As a result, the system spontaneously resides into a stable and usually spatially periodic concentration distribution. The WP model is one of the classic models for polarization. It is similar to the Turing mechanism, but does not result in periodic patterns. It usually involves one molecular species with two different forms, which also have distinct diffusion constants. The underlying mechanism is similar to the wave front solution of spatially coupled systems, but with the wave speed controlled by one of its molecular forms.[14] The steady-state pattern is reached when the wave speed equals zero, i.e., "pinning". The characteristic feature of the AT model is that molecules are actively transported, e.g., via dynein-mediated active transportation,[15–17] toward some direction. The balance between active transportation and passive diffusion determines the steady-state concentration distribution, which is generally nonuniform. The SDD model is one of the most studied mechanisms for morphogen gradients.[4,7,18] It involves the synthesis, degradation, and passive diffusion of one molecular species. The synthesis term is usually considered as a spatially fixed source. The balance between these three effects determines the steady-state pattern. For the classic SDD model with a single point synthesis source and linear degradation, the steady-state solution can be well described by an exponential profile.

Recently, optimal information transmission from morphogen gradients to their downstream genes has been studied from various aspects. For instance, studies have demonstrated that specific morphogen gradients can be optimized to minimize downstream gene expression noise or maximize the mutual information between morphogen concentration and downstream gene expression.[19–21] Furthermore, the suppression of gradient noise is associated with the cost of increasing molecular concentration.[22] Nevertheless, the direct impact of the diffusion effect on information transmission processes remains unclear. A systematic investigation across models is still lacking.

Since diffusion is a dissipative random effect, it might be expected that diffusion could be detrimental to information transmission.[13,22] However, it is well known that the Tur-

†Corresponding author. E-mail: liufeng@hebut.edu.cn
© 2024 Chinese Physical Society and IOP Publishing Ltd

ing instability necessitates the involvement of diffusion, implying that such randomness could induce global order, resembling the theory of stochastic resonance.[23–26] Nonetheless, how diffusion affects the positional information of spatial concentration patterns in general, especially for mechanisms other than the Turing mechanism,[7,13,19,20,22] remains to be explored. Therefore, this study focuses on the other three representative models: the AT, SDD, and WP models.

In this paper, we first analyze the general relation between the diffusion constant (D) and the amount of positional information (PI) in one-dimensional systems, and show that a nonmonotonic relationship is expected. We further validate this relationship with numerical simulations in three distinct patterning mechanisms including the AT, SDD, and WP models. Our results demonstrate that all three representative models produce nonmonotonic curves of PI versus D, despite their differences in patterning dynamics. Moreover, we relate PI to the thermodynamic energy required to resist the dissipation of diffusion (ΔS) to understand the physical constraints of positional information transmission in patterning systems. We find that the nonmonotonicity disappears when the total energy is constrained. Furthermore, an upper limit of PI, depending on the energy dissipation, is observed, which matches the theoretical derivation. Specifically, the relationship between the maximal PI and ΔS is consistent across models, irrespective of their details.

2. Results and discussion

To study the general relationship between D and PI, we first analytically study one-dimensional patterning systems. Such patterning systems can be described using a partial differential equation as

$$\partial_t c = D\partial_x^2 c + g, \tag{1}$$

where $c = c(x,t)$ is the concentration of the patterning molecule of interest, $x \in [0,L]$ where L is the length of the system, and $g = g(x,c,\partial_x c)$ is the general force including the transport, production or degradation of the patterning molecules. At a steady-state, the concentration distribution is denoted as: $c_{ss} = Nf(x)$, where $N = \int c_{ss}(x)\,\mathrm{d}x$ is the total number of molecules, $f(x) = c_{ss}(x)/N$ is the probability density function of a molecule along the spatial dimension.

The readout of the steady-state concentration $\hat{c}$, e.g., by a cell, is generally noisy. According to the Berg–Purcell limit,[27–31] this noise has a physical lower bound as

$$\sigma_{\hat{c}}^2 = \left\langle (\hat{c} - c_{ss})^2 \right\rangle \geq \varepsilon \frac{c_{ss}}{DT}, \tag{2}$$

where ε is a constant depending on the details of the readout mechanism such as the receptor size, the value of ε depends on the unit of c, and T is the readout time span.

Despite the readout noise of the concentration, it is theoretically possible that the cell position x can be estimated to some extent based on the readout of the local concentration. Theoretically, the amount of information about x that can be extracted by reading the concentration is quantified by the mutual information between x and $\hat{c}$, denoted as PI,[8,9] which is defined as

$$PI = I\left(X;\hat{C}\right) = H(X) - H\left(X|\hat{C}\right) = H\left(\hat{C}\right) - H\left(\hat{C}|X\right), \tag{3}$$

where H denotes the differential entropy, e.g., $H\left(\hat{C}\right) = -\int p_{\hat{C}}(\hat{c}) \ln p_{\hat{C}}(\hat{c})\,\mathrm{d}\hat{c}$ determined by the probability density function of $\hat{c}$, $p_{\hat{C}}(\hat{c})$, and similarly for $H(X)$, the conditional differential entropy is defined as, e.g.,

$$H\left(\hat{C}|X\right) = -\int p_X(x) \int p_{\hat{C}|X}(\hat{c}\,|x) \ln p_{\hat{C}|X}(\hat{c}|x)\,\mathrm{d}\hat{c}\,\mathrm{d}x,$$

and similarly for $H\left(X|\hat{C}\right)$. Following the convention in information theory, the random variables X and $\hat{C}$ are used to denote the mutual information $I\left(X;\hat{C}\right)$, and similarly for the differential entropy, emphasizing that it is not a function of the values of such random variables x or $\hat{c}$.

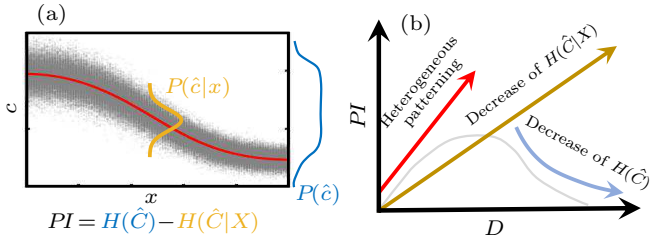


Fig. 1. The PI of a spatial concentration pattern is affected by D. (a) PI quantified by the mutual information between the position coordinate x and the readout concentration $\hat{c}$, is the difference between the concentration's global uncertainty $H(\hat{C})$ and local uncertainty $H\left(\hat{C}|X\right)$. (b) Multiple effects influence PI. The heterogeneous patterning requires nonzero diffusion (red arrow). The local uncertainty, i.e., the readout noise of concentration, is reduced by increasing diffusion according to the Berg–Purcell limit (brown arrow). The global uncertainty is reduced if the diffusion effect is too strong and the pattern becomes too flat (blue arrow). As a result, a nonmonotonic relationship between D and PI is expected (gray curve).

According to Eq. (3), PI is a combined effect of the concentration's global uncertainty $H\left(\hat{C}\right)$, and local uncertainty $H\left(\hat{C}|X\right)$ (Fig. 1(a)). Intuitively, the establishment of the spatial pattern requires a nonzero D, therefore increasing D at $D \sim 0$ could increase PI (Fig. 1(b)). Furthermore, increasing D can decrease the readout noise (Eq. (2)) and, therefore, decrease $H\left(\hat{C}|X\right)$, leading to the increase of PI (Fig. 1(b)). However, increasing D simultaneously flattens the concentration distribution when D is high (Eq. (1)), which decreases $H\left(\hat{C}\right)$ and therefore PI (Fig. 1(b)). In fact, as an extreme condition, $c_{ss}(x)$ is a constant as $D \to \infty$, thus $PI(D \to \infty) = PI(D = 0) = 0$. Combining these effects would lead to a nonmonotonic relationship between D and PI (Fig. 1(b)). Next, we mathematically validate these intuitions.

Mathematically, when $D \to 0$, the concentration readout noise Eq. (2) diverges and, therefore, $\sigma_{\hat{c}}^2 \gg (\partial_x c)^2 L^2$, which,

in turn, yields $H\left(\hat{C}|X\right) \approx H\left(\hat{C}\right) \to +\infty$, i.e., the global uncertainty $H\left(\hat{C}\right)$ is dominated by the readout noise $\sigma_{\hat{c}}^2$ rather than the nonuniform distribution $(\partial_x c)^2 L^2$. Under this condition, the positional information is $PI = H\left(\hat{C}\right) - H\left(\hat{C}|X\right) \approx 0$. In other word, PI positively correlates with D at $D \approx 0$:

$$\left(\frac{\mathrm{d}}{\mathrm{d}D}PI\right)_{D\approx 0} > 0. \tag{4}$$

When D is relatively large and readout noise is small such that $\sigma_{\hat{c}}^2 \ll (\partial_x c)^2 L^2$, approximately we have $p_{\hat{c}}(\hat{c}) \approx \frac{p_x(x)}{|\mathrm{d}c_{\mathrm{ss}}/\mathrm{d}x|}$, and the global uncertainty is thus

$$\begin{aligned} H\left(\hat{C}\right) &= H(X) + \frac{1}{2}\left\langle \ln\left(\frac{\mathrm{d}c_{\mathrm{ss}}}{\mathrm{d}x}\right)^2 \right\rangle_x \\ &\approx H(X) + \frac{1}{2}\left\langle \ln\left(\frac{\mathrm{d}c_0}{\mathrm{d}x}\right)^2 \right\rangle + \left\langle \frac{\mathrm{d}\Delta c/\mathrm{d}x}{\mathrm{d}c_0/\mathrm{d}x} \right\rangle, \end{aligned}$$

where $c_{\mathrm{ss}}(x) = c_0(x) + \Delta c(x)$ with the concentration change $\Delta c \ll c_0$ due to the change of diffusion constant $D = D_0 + \Delta D$. To estimate the term $\left\langle \frac{\mathrm{d}\Delta c/\mathrm{d}x}{\mathrm{d}c_0/\mathrm{d}x} \right\rangle$, substituting $D = D_0 + \Delta D$ and $c_{\mathrm{ss}}(x) = c_0(x) + \Delta c(x)$ into Eq. (1) under the steady-state condition $\partial_t c = 0$ and focus on the diffusion effect, approximately we have

$$D\frac{\mathrm{d}^2\Delta c}{\mathrm{d}x^2} + \Delta D\frac{\mathrm{d}^2 c_0}{\mathrm{d}x^2} \approx 0, \tag{5}$$

where an assumption is made that the change of the concentration distribution Δc does not affect the general force g, since we restrain our focus on the diffusion effect. This assumption may not be rigorous but it helps gain insight to the *D*–*PI* relationship. Integrating Eq. (5) from 0 to x and using the zero-flux boundary condition at $x = 0$ yields

$$D_0\frac{\mathrm{d}\Delta c}{\mathrm{d}x} + \Delta D\frac{\mathrm{d}c_0}{\mathrm{d}x} = 0, \tag{6}$$

substituting this equation into the expression of $H\left(\hat{C}\right)$ yields

$$H\left(\hat{C}\right) \approx H_0\left(\hat{C}\right) - \frac{\Delta D}{D_0}, \tag{7}$$

where

$$H_0\left(\hat{C}\right) = H(X) + \frac{1}{2}\left\langle \ln\left(\frac{\mathrm{d}c_0}{\mathrm{d}x}\right)^2 \right\rangle.$$

Regarding the local uncertainty $H\left(\hat{C}|X\right)$, since the concentration readout is based on molecule counting, the conditional distribution $p_{\hat{C}|X}(\hat{c}|x)$ is approximately Gaussian according to the central limit theorem when D is large enough. Therefore,

$$\begin{aligned} H\left(\hat{C}|X\right) &\approx \frac{1}{2}\left\langle \ln 2\pi e\sigma_{\hat{c}}^2 \right\rangle_x \\ &= \frac{1}{2}\ln\frac{2\pi e\varepsilon}{T} + \frac{1}{2}\left\langle \ln\frac{c_0}{D_0} \right\rangle_x + \frac{1}{2}\left\langle \frac{\Delta c}{c_0} \right\rangle_x - \frac{1}{2}\frac{\Delta D}{D_0}. \end{aligned}$$

The term $\left\langle \Delta c/c_0 \right\rangle_x$ is estimated as follows: equation (6) is first integrated from an arbitrary x_c to x, yields:

$$D_0\left[\Delta c - \Delta c_c\right] + \Delta D\left[c_0 - c_{0c}\right] = 0, \tag{8}$$

where $c_{0c} = c_0(x_c)$, and $\Delta c_c = \Delta c(x_c)$. By assuming that the diffusion effect does not affect N, we can apply a constraint $\langle \Delta c \rangle = (1/L)\int \Delta c(x)\,\mathrm{d}x = 0$, where the prior distribution of cell positions is uniform $p_X(x) = 1/L$. Noticeably, N could depend on D in some patterning systems such as the Turing system with strong nonlinear regulations.[12,13] However, such systems could mix the effect of diffusion, molecule number and energy requirement, introducing unnecessary complexity in this analysis, hence here we only focus on patterning systems in which N is not affected by changing D (the effect of the molecule number is discussed along with the energy requirement later). Therefore, equation (8) gives $0 = D_0\langle \Delta c \rangle = -\Delta D\langle c_0 \rangle + \Delta D c_{0c} + D_0 \Delta c_c$, thus

$$\left\langle \frac{\Delta c}{c_0} \right\rangle = \frac{\Delta D}{D_0}\left\langle \frac{\langle c_0 \rangle - c_0}{c_0} \right\rangle = \gamma\frac{\Delta D}{D_0},$$

where $\gamma = \left\langle \frac{\langle c_0 \rangle - c_0}{c_0} \right\rangle \geq 0$. Substituting this relation into the expression of $H\left(\hat{C}|X\right)$ yields

$$H\left(\hat{C}|X\right) = H_0\left(\hat{C}|X\right) + \frac{\gamma}{2}\frac{\Delta D}{D_0} - \frac{1}{2}\frac{\Delta D}{D_0}, \tag{9}$$

where $H_0\left(\hat{C}|X\right)$ is the local uncertainty when $D = D_0$.

Thus when D is large, PI is given by combining Eqs. (7) and (9)

$$PI = H\left(\hat{C}\right) - H\left(\hat{C}|X\right) = PI_0 - \frac{\gamma + 1}{2}\frac{\Delta D}{D_0}. \tag{10}$$

Therefore, we have $\frac{\mathrm{d}}{\mathrm{d}D}PI < 0$ when D is large.

Taken Eqs. (4) and (10) together, as $PI \geq 0$, the relationship between D and PI must be nonmonotonic (Fig. 1(b)).

So far, we have analytically justified that a nonmonotonic relationship between D and PI is expected for concentration patterning systems. However, simplifications are involved in the derivation, and the details of the *D*–*PI* relationship remain vague. Therefore, we next resort to numerical simulations to quantify the *D*–*PI* curve for specific patterning systems.

For simplicity, we apply a simplified AT model to illustrate the *D*–*PI* relationship. In the simplified AT model, the molecule number is conservative, and the general force term in Eq. (1) is now $g = -k\partial_x c$, where $k > 0$ is the flux intensity toward $x = 0$. Numerical simulations of this model, assuming the noise follows Eq. (2) with varying D, reveal a nonmonotonic relationship between D and PI (Fig. 2). The mutual information is estimated based on the k-nearest neighbor method.[32] We also test the relationship under different noise intensity ε; the nonmonotonicity is preserved with deformation of the curve (Fig. 2(b)). The optimal diffusion constant corresponding to the maximal PI remains largely the same,

which corresponds to a length constant of $D/k \sim 0.3L$, similar to that of the SDD model (see Appendix A for details). This similarity in the optimal decay length is not surprising because the patterns of the AT model and the SDD model are both exponential-like, while *PI* relies solely on the shape of the pattern and readout noise. Furthermore, we confirm that other models yield similar conclusions including the SDD model and the WP model (see Appendices A and B for details). These results suggest that diffusion, as a random effect, can increase the information transmission, resembling the phenomenon of stochastic resonance.[23]

In these simulations, the values of ε are selected so that the maximal value of *PI* falls within the biologically relevant range, i.e., $PI \gtrsim 2$ nats ≈ 3 bits. For instance, it is estimated that a minimal requirement of positional information is approximately 4 bits for the precise development of the anterior-posterior patterning of early fly embryos.[9] Nevertheless, we further confirm that the nonmonotonic relationship remains in simulations with extended ranges of ε and D (Fig. C1, see Appendix C for details).

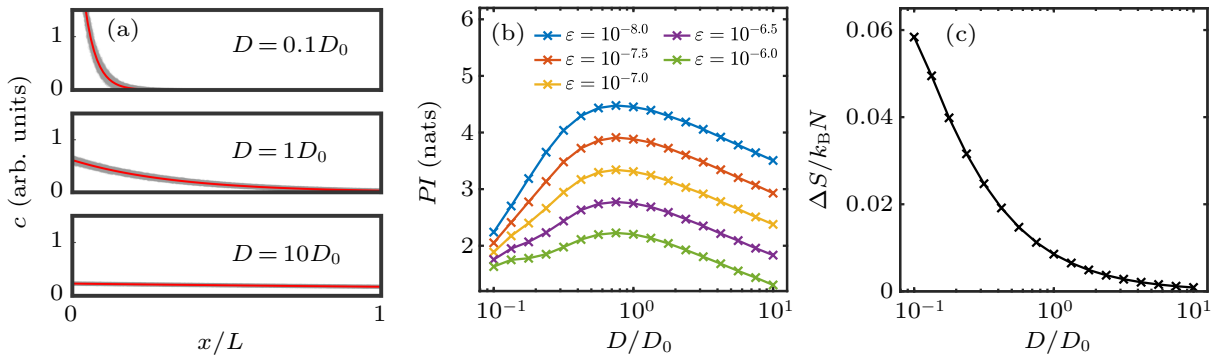


Fig. 2. Numerical simulation results of *PI* of the AT model. (a) The steady-state concentration distribution under different D with $\varepsilon = 10^{-6}$. Large D results in a small readout noise but leads to a flatter distribution (top to bottom). (b) The nonmonotonic relationship between D and *PI* in the simulation of the AT model. Different noise amplitudes ε, across two orders of magnitude, are tested. (c) The entropy production, equivalent to the energy requirement for maintaining the pattern, depends on D monotonically within the range tested. The parameters of the model are as follows: $k = 0.003$, $D_0 = 10^{-3}$, and $L = 1$ for the AT model, the reading timespan is $T = 1$. The unit of c in the simulation is arbitrary with $\int_0^1 c\,\mathrm{d}x = 0.2$.

To understand the underlying physical constraints of the positional information, we next examine the energy dissipation in these patterning systems.

Since diffusion is a dissipative random process, maintaining such an informative spatial distribution of molecules involves energy dissipation. What is the relationship between energy dissipation, the diffusion constant, and positional information? While the dissipation of the active force depends on the reversibility details of the underlying mechanisms, the dissipation of the diffusion process is universal and is theoretically tractable. The Gibbs entropy of a steady-state distribution $c_{\mathrm{ss}}(x) = Nf(x)$ is given by $S = -Nk_{\mathrm{B}}\int f(x)\ln f(x)\,\mathrm{d}x$. Combining this with the evolution of the distribution, as described by Eq. (1), under the steady-state we have

$$\begin{aligned}\dot{S} &= \dot{S}_{\mathrm{diff}} + \dot{S}_{\mathrm{g}} \\ &= -Nk_{\mathrm{B}}\int (1+\ln f)\cdot\left(D\frac{\mathrm{d}^2 f}{\mathrm{d}x^2}\right)\mathrm{d}x \\ &\quad -Nk_{\mathrm{B}}\int (1+\ln f)\cdot\frac{g}{N}\,\mathrm{d}x = 0.\end{aligned}$$

Therefore, the entropy production rate due to diffusion, or equivalently, the energy required to counteract diffusion dissipation, is

$$\dot{S}_{\mathrm{diff}} = k_{\mathrm{B}}DN\int \frac{(\mathrm{d}f/\mathrm{d}x)^2}{f}\,\mathrm{d}x \geq 0. \tag{11}$$

This rate depends on the shape of the concentration distribution and the total number of molecules. Equation (11) defines a lower limit of the free energy required to maintain an informative concentration distribution for a time duration T as follows:

$$\Delta S = \dot{S}_{\mathrm{diff}}T = k_{\mathrm{B}}DNT\int \frac{(\mathrm{d}f/\mathrm{d}x)^2}{f}\,\mathrm{d}x$$

under the unit that temperature equals 1, i.e., maintaining such a distribution requires at least the same amount of energy dissipated by diffusion.

In the simulations of the AT model, the relationship between D and ΔS appears to be monotonic within the range of D tested (Fig. 2(c)). However, for the SDD model and the WP model, this relationship is nonmonotonic near the optimal value of D (see Appendices A and B for details). These results suggest that there is no general relationship between D and ΔS. An immediate question is whether the positional information encoded by a stable concentration distribution is limited by the energy it dissipates.

To gain insight into the relationship between ΔS and *PI*, akin to the derivation of Eq. (10), we assume $p_{\hat{c}}(\hat{c}\,|\,x)$ is a Gaussian distribution and $\sigma_c^2 \ll (\mathrm{d}c/\mathrm{d}x)^2 L^2$ focusing on the large D regime. Under these assumptions, the global uncer-

tainty follows

$$H\left(\hat{C}\right) = H\left(X\right) + \left\langle \frac{1}{2}\ln\left(N\frac{\mathrm{d}f}{\mathrm{d}x}\right)^2 \right\rangle_x,$$

where $H\left(X\right) = \ln L$ assuming the prior distribution of the cell position is uniform $p_X\left(x\right) = 1/L$. The local uncertainty follows

$$\begin{aligned} H\left(\hat{C}|X\right) &= \left\langle \frac{1}{2}\ln 2\pi e\sigma_{\hat{c}}^2 \right\rangle_x \\ &= \frac{1}{2}\ln 2\pi e + \left\langle \frac{1}{2}\ln \varepsilon N\frac{f}{DT} \right\rangle_x. \end{aligned}$$

The positional information is thus

$$\begin{aligned} PI &= H\left(\hat{C}\right) - H\left(\hat{C}|X\right) \\ &= \frac{1}{2}\ln\frac{L}{2\pi e\varepsilon} + \left\langle \frac{1}{2}\ln LNDT\frac{\left(\mathrm{d}f/\mathrm{d}x\right)^2}{f} \right\rangle_x. \end{aligned} \tag{12}$$

Noting that $\langle \ln\cdots\rangle \leq \ln\langle\cdots\rangle$, combining this with Eq. (11) yields an inequality

$$PI \leq \frac{1}{2}\ln\frac{L}{2\pi e\varepsilon} + \frac{1}{2}\ln\frac{\Delta S}{k_{\mathrm{B}}}. \tag{13}$$

Equation (13) indicates that the positional information encoded by a concentration distribution of molecules is physically constrained by the energy required for maintaining such nonuniform distribution.

To numerically analyze the relationship between ΔS and PI, we introduce a parameter α, quantifying the fold-change of the total molecule number of the pattern while keeping the shape of the steady-state distribution unchanged, as another dimension of tuning the energy and modify Eq. (1) as

$$\frac{\partial\tilde{c}}{\partial t} = D\frac{\partial^2\tilde{c}}{\partial x^2} + g, \tag{14}$$

where $\tilde{c} = c/\alpha$. The steady-state distribution is now $c_{\mathrm{ss}}\left(x\right) = \alpha N_0 f\left(x\right)$, and the total number of molecules is now $\int c_{\mathrm{ss}}\left(x\right)\mathrm{d}x = \alpha N_0$, N_0 corresponds to the number of molecule when $\alpha = 1$. The normalized shape of the spatial distribution $f\left(x\right)$ does not change when tuning α and fixing D, therefore the energy requirement is now $\Delta S = \alpha\Delta S_0(D)$, where $\Delta S_0\left(D\right)$ is the energy requirement when $\alpha = 1$ given D. We then analyze the relation between the diffusion constant, positional information, and energy requirement by screening the two parameters D and α.

In the simulations of the AT model, while a nonmonotonic relationship between D and PI is observed when α is fixed (Fig. 3(a)), the D–PI relationship becomes nearly monotonic with an asymptotic maximal value when ΔS is fixed (Fig. 3(b)). This matches the theoretical result (Eq. (13)) which predicts that when D is large, PI depends solely on ΔS. Moreover, by combining the simulation results of screening α and D, we observed a clear upper bound on the scatter plot of PI versus ΔS, following $PI \sim 0.48\ln\Delta S$ (Fig. 4). This suggests that the amount of positional information provided by a spatially heterogeneous pattern is limited by the energy dissipation of such a pattern, as predicted by Eq. (13). Similar results are observed in the simulations of the SDD and WP models (see Appendices A and B for details). The discrepancy between the slope of the theoretical upper bound and the simulation result might stem from the oversimplification in deriving Eq. (13), and the condition for $\langle \ln\cdots\rangle = \ln\langle\cdots\rangle$ is not satisfied in the simulated pattern.

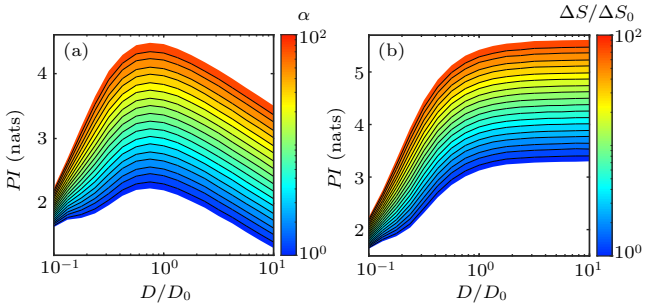


Fig. 3. The relationship between D and PI under different constraints with $\varepsilon = 10^{-6}$. (a) When constraining the molecular number, quantified by its fold change $\alpha = N/N_0$, the relationship between D and PI is strongly nonmonotonic. (b) When constraining the energy dissipation level ΔS, the relationship between D and PI becomes monotonic with an asymptotic maximum.

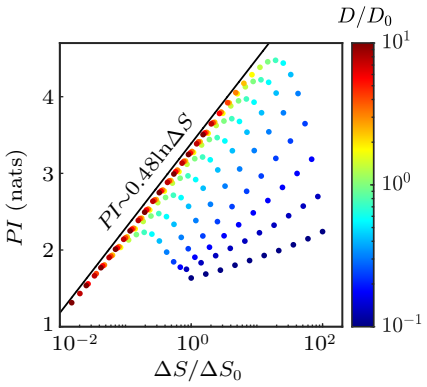


Fig. 4. The relationship between ΔS and PI. In the simulation of the AT model with varying D and molecule numbers α (dots), the ΔS–PI data exhibit an upper bound (illustrated by the black line).

While our focus is on the physical aspect of spatial patterning, other factors governing patterning, such as the active transport process or chemical reactions in the SDD model, could also have comparable effects on PI. However, since the noise from such processes and its connection to energy dissipation depend heavily on the ad hoc details of the underlying reversibility properties, deriving a general rule on how they affect information remains challenging. Hence, we only consider the physical effects in this paper. Nevertheless, our results provide a fundamental constraint: the actual information encoded in a pattern can never exceed the one we calculate, and the actual energy dissipation cannot be less than our calculated level (Eq. (13)).

In this paper, we examined three representative minimal models of patterning to investigate the relationship between diffusion and positional information. We believe our study can not only deepen our understanding of natural patterning systems but also highlight an important, yet perhaps overlooked, aspect of designing synthetic morphogenesis — an active area in synthetic biology.[33] While real biological systems are typically more complex than these models, considering such complexity is beyond the scope of the current study, as it may hinder the understanding of the physical relationship between D and PI. However, recently, implicit evidence has suggested that the nonmonotonic relationship between D and PI also exists in complex multi-mode regulatory networks,[34] without a detailed investigation into the mechanism. Thus, it remains important to generalize our findings to complex systems.

3. Conclusion

In conclusion, we explored the physical constraints on positional information in spatial patterning. Specifically, we found that the diffusion process, being dissipative, affects positional information in a nonmonotonic manner. Furthermore, we illustrated the connection between positional information and the physical energy dissipation required to maintain such patterns. We presented an upper limit for positional information given a certain energy level.

Appendix A: Synthesis-degradation-diffusion (SDD) model

Similar to the AT model, the SDD model is also a one-dimensional system following

$$\partial_t c = D\partial_x^2 c - \beta c + j(x),$$

where $j(x)$ is the synthesis term with $j\ (x \le 0.1) = 0.02$, $j\ (x > 0.1) = 0$, and $\beta = 0.01$ is the degradation rate. The initial condition of the SDD model is arbitrary. A nonmonotonic D–PI relationship is observed in the numerical results (Fig. A1). Similar to the AT model, the optimal diffusion constant remains largely unchanged with different ε, corresponding to a length constant of $\sqrt{D/\beta} \sim 0.3L$.

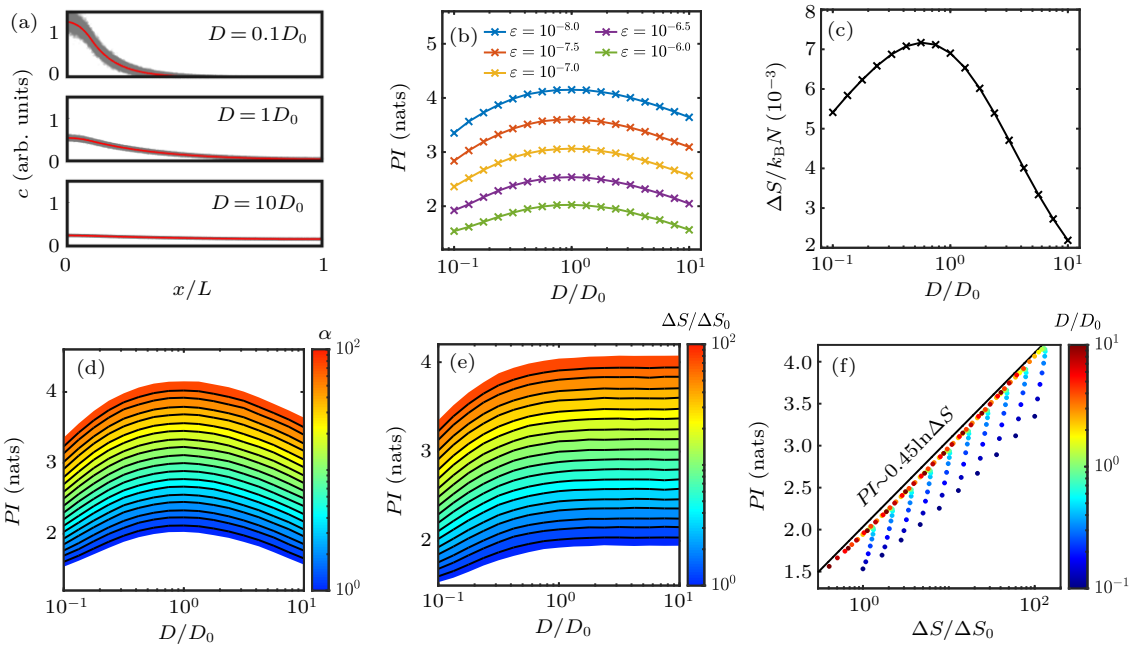


Fig. A1. Numerical simulation results of the SDD model. (a) The steady-state concentration distribution under different diffusion constants with $\varepsilon = 10^{-6}$. Similar to Fig. 2(a) in the main text. (b) The nonmonotonic D–PI relationship in the simulation of the SDD model. Different noise amplitudes ε are tested as in Fig. 2(b) in the main text. (c) The energy requirement for maintaining the pattern also depends on the diffusion constant nonmonotonically in the SDD model. (d) The D–PI relation is still nonmonotonic when constraining α. (e) The D–PI relationship turns into monotonic with an asymptotic maximum when constraining the energy. (f) An upper bound of PI following $PI \sim 0.45 \ln \Delta S$ is observed for the SDD model. In the numerical simulation, $D_0 = 10^{-3}$ and $T = 1$.

Appendix B: The wave-pinning (WP) model

The WP model follows[14]

$$\begin{cases} \partial_t c_1 = \left(v_0 + \dfrac{v c_1^2}{K^2 + c_1^2}\right) c_2 - \beta c_1 + D\partial_x^2 c_1, \\ \partial_t c_2 = -\left(v_0 + \dfrac{v c_1^2}{K^2 + c_1^2}\right) c_2 + \beta c_1 + D_2 \partial_x^2 c_2, \end{cases}$$

where c_1 is the concentration of the patterning molecule, c_2 is a fast diffusion molecule, i.e., $D_2 \gg D_1$, which is approximated as a uniform distribution throughout the simulation. $v_0 = 0.006$, $v = 0.1$, $K = 1$, and $\beta = 0.1$. The initial condition of the WP model is $c_1\ (x < 0.2) = 1.29$, $c_1\ (x \ge 0.2) = 0$, and $c_2\ (x) = 2.15$. A nonmonotonic D–PI relationship is observed in the numerical results (Fig. B1).

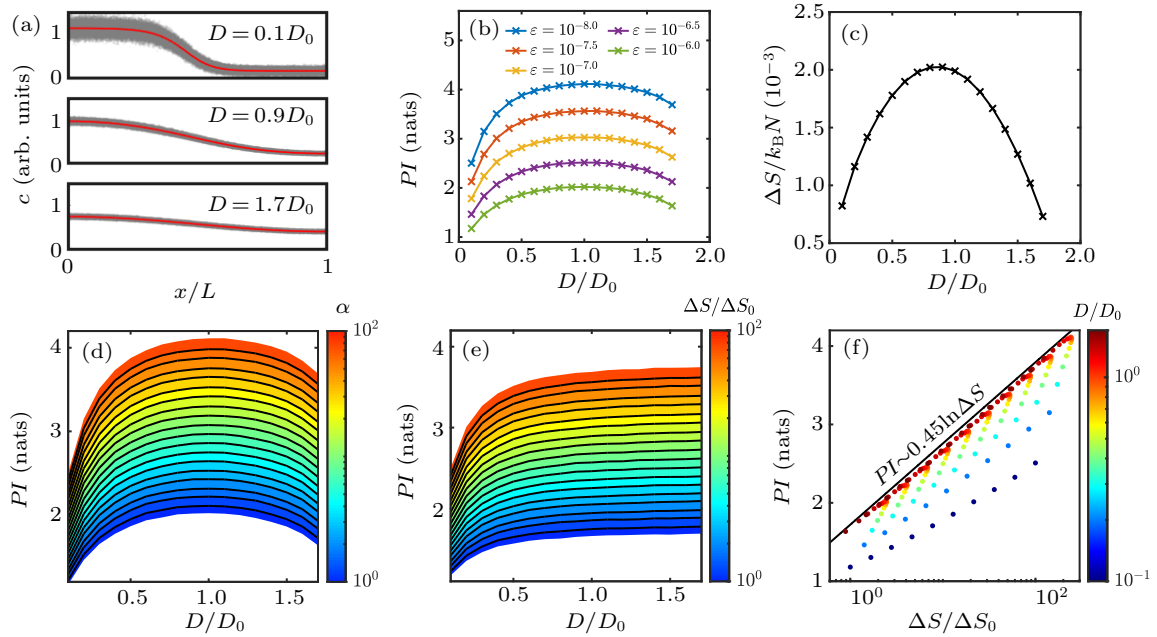


Fig. B1. Numerical simulation results of the WP model. (a) The steady-state concentration distribution under different diffusion constants with $\varepsilon = 10^{-6}$. (b) The nonmonotonic *D*–*PI* relationship in the simulation of the WP model. Different noise amplitudes ε are tested. (c) The energy requirement for maintaining the pattern also depends on the diffusion constant nonmonotonically in the WP model. (d) The *D*–*PI* relationship is still nonmonotonic when constraining α. (e) The *D*–*PI* relationship turns into monotonic with an asymptotic maximum when constraining the energy. (f) An upper bound of *PI* following $PI \sim 0.45 \ln \Delta S$ is observed for the WP model. In the numerical simulation, $D_0 = 10^{-3}$ and $T = 1$.

Appendix C: Simulations with extended parameter ranges

In the main text and Appendices A and B, the simulation of the three models is performed with the range of ε being 10^{-8}–10^{-6}, and the range of D/D_0 being 10^{-1}–10^{1}. Extending the ranges of these parameters does not affect the conclusions. Although further increasing the noise amplitude ε results in nearly non-informative concentration distributions, it is theoretically worth analyzing such an extreme condition.

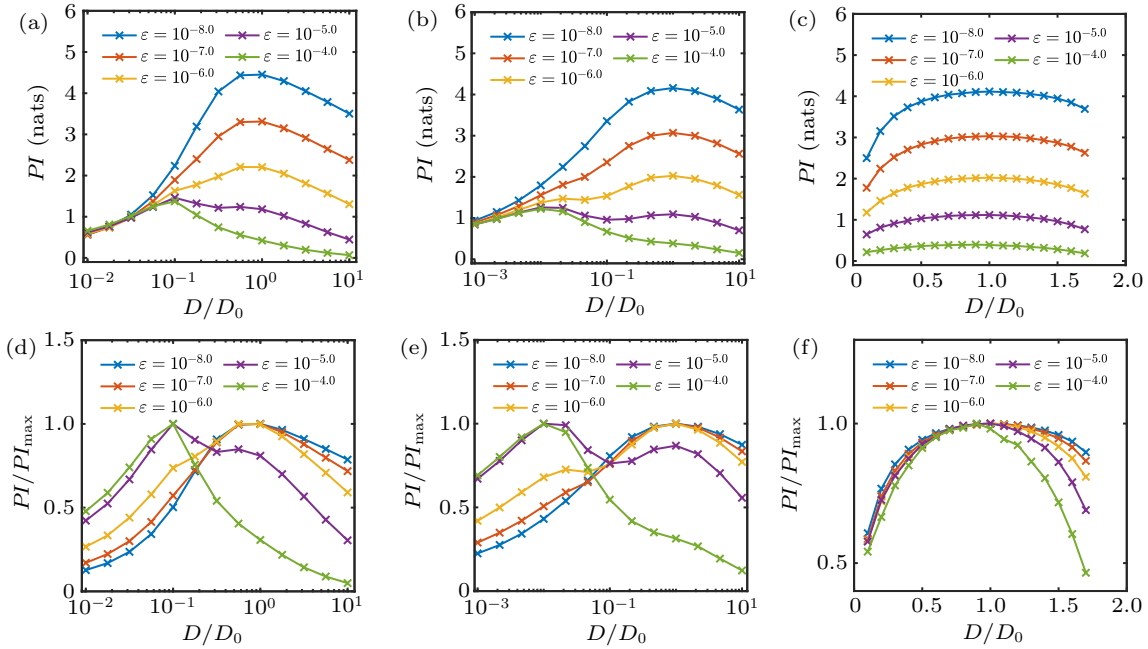


Fig. C1. Numerical simulation results of the AT model [panels (a) and (d)], SDD model [panels (b) and (e)], and WP model [panels (c) and (f)] in extended parameter ranges. Panels (a)–(c) are the D/D_0–*PI* relationship for the three models when increasing the noise amplitude ε. Panels (d)–(f) are the D/D_0–$PI/PI_{\rm max}$ relationship for the three models when increasing the noise amplitude ε.

Specifically, we confirm that the nonmonotonicity between *D* and *PI* remains if the value of ε is increased by two orders of magnitude to 10^{-4} for all three models (Figs. C1(a)–C1(c)). However, a significant shift of the optimal diffusion constant is observed in the AT and SDD models (Figs. C1(a) and C1(b)), but not in the WP model (Fig. C1(c)). The dif-

ferent structure of the *D–PI* curve is a consequence of the differences in model details. For both the AT and SDD models, since the concentration distribution with $D \to 0$ is a delta function-like shape with an extremely large dynamic range, *PI* could remain a non-zero value even when extremely high noise is presented. Hence, a smaller optimized *D* could result in a greater *PI* reading from a steeper concentration distribution. However, although the concentration distribution of the WP model when $D \to 0$ can also be a step function-like shape, its dynamic range does not increase. Therefore, extremely high noise monotonically decreases *PI* without significantly affecting the optimal *D* for the WP model.

Moreover, the *D–PI* relationship for the three models remains highly nonmonotonic even with extremely high noise. Specifically, although the *D–PI* curve appears flattened in absolute units of *PI* when increasing ε, normalized *PI* by its maximal value shows that the nonmonotonicity is preserved (Figs. C1(d)–C1(f)).

Acknowledgement

Project supported by the National Natural Science Foundation of China (Grant Nos. 32271293 and 11875076).

References

[1] Lander A D 2013 *Science* **339** 923
[2] Lewis J, Slack J M W and Wolpert L 1977 *J. Theor. Biology* **65** 579
[3] Yang Z, Wu X, Yang N and Liu F 2018 *Quantitative Biology* **6** 15
[4] Rogers K W and Schier A F 2011 *Annual Review of Cell and Developmental Biology* **27** 377
[5] Muller P, Rogers K W, Yu S R, Brand M and Schier A F 2013 *Development* **140** 1621
[6] Vetter R and Iber D 2022 *Nat. Commun.* **13** 1145
[7] Fancher S and Mugler A 2020 *eLife* **9** 1
[8] Tkačik G, Dubuis J O, Petkova M D and Gregor T 2015 *Genetics* **199** 39
[9] Dubuis J O, Tkacik G, Wieschaus E F, Gregor T and Bialek W 2013 *Proc. Natl. Acad. Sci. USA* **110** 16301
[10] Tkačik G and Gregor T 2021 *Development* **148** dev176065
[11] Bauer M, Petkova M D, Gregor T, Wieschaus E F and Bialek W 2021 *Proc. Nat. Acad. Sci. USA* **118** e2109011118
[12] Murray S M and Sourjik V 2017 *Nat. Phys.* **13** 1006
[13] Zhang D, Zhang C, Ouyang Q and Tu Y 2023 *J. R. Soc. Interface.* **20** 20230276
[14] Mori Y, Jilkine A and Edelstein-Keshet L 2008 *Biophys. J.* **94** 3684
[15] Stapornwongkul K S and Vincent J P 2021 *Nature Reviews Genetics* **22** 393
[16] Weil T T, Forrest K M and Gavis E R 2006 *Developmental Cell* **11** 251
[17] Reck-Peterson S L, Redwine W B, Vale R D and Carter A P 2018 *Nat. Rev. Mol. Cell Biol.* **19** 382
[18] Berezhkovskii A M, Sample C and Shvartsman S Y 2010 *Biophys. J.* **99** L59
[19] Emberly E 2008 *Phys. Rev.E* **77** 041903
[20] Saunders T E and Howard M 2009 *Phys. Rev. E* **80** 041902
[21] Sokolowski T R and Tkačik G 2015 *Phys. Rev. E* **91** 062710
[22] Song Y and Hyeon C 2021 *eLife* **10** e70034
[23] McDonnell M D and Abbott D 2009 *PLoS Comput Biol* **5** e1000348
[24] Tottori T, Fujii M and Kuroda S 2019 *Phys. Rev. E* **100** 042403
[25] Martineau S, Saffold T, Chang T T and Ronellenfitsch H 2022 *Phys. Rev. Lett.* **128** 98301
[26] Nicolaou Z G, Sebek M, Kiss I Z and Motter A E 2020 *Phys. Rev. Lett.* **125** 094101
[27] Berg H C and Purcell E M 1977 *Biophys. J.* **20** 193
[28] Kaizu K, de Ronde W, Paijmans J, Takahashi K, Tostevin F and ten Wolde P R 2014 *Biophys. J.* **106** 976
[29] Ten Wolde P R, Becker N B, Ouldridge T E and Mugler A 2016 *J. Stat. Phys.* **162** 1395
[30] Bialek W and Setayeshgar S 2005 *Proc. Natl. Acad. Sci. USA* **102** 10040
[31] Gregor T, Tank D W, Wieschaus E F and Bialek W 2007 *Cell* **130** 153
[32] Kraskov A, Stögbauer H and Grassberger P 2004 *Phys. Rev. E* **69** 066138
[33] Grant P K, Szep G, Patange O, Halatek J, Coppard V, Csikász-Nagy A, Haseloff J, Locke J C W, Dalchau N and Phillips A 2020 *Nat. Commun.* **11** 5545
[34] Sokolowski T R, Gregor T, Bialek W and Tkačik G 2023 arXiv: 2302.05680 [physics.bio-ph]